

3-kHz Er:YAG single-frequency laser with a ‘triple-reflection’ configuration on a piezoelectric actuator

Shuai Huang(黄帅), Qing Wang(王庆), Meng Zhang(张濛), Chaoyong Chen(陈朝勇), Kaixin Wang(王凯鑫), Mingwei Gao(高明伟), Chunqing Gao(高春清)
Citation: Chin. Phys. B . 2020, 29(8): 084204 . **doi:** 10.1088/1674-1056/ab9441
Journal homepage: http://cpb.iphy.ac.cn; http://iopscience.iop.org/cpb

What follows is a list of articles you may be interested in

Stable continuous-wave single-frequency intracavity frequency-doubled laser with intensity noise suppressed in audio frequency region

Ying-Hao Gao(高英豪), Yuan-Ji Li(李渊骥), Jin-Xia Feng(冯晋霞), Kuan-Shou Zhang(张宽收)
Chin. Phys. B . 2019, 28(9): 094204 . **doi:** 10.1088/1674-1056/ab327b

Fe: ZnSe laser pumped by a 2.93-μm Cr, Er: YAG laser

Ying-Yi Li(李英一), Tong-Yu Dai(戴通宇), Xiao-Ming Duan(段小明), Chun-Fa Guo(郭春发), Li-Wei Xu(徐丽伟), You-Lun Ju(鞠有伦)
Chin. Phys. B . 2019, 28(6): 064203 . **doi:** 10.1088/1674-1056/28/6/064203

Development of an injection-seeded single-frequency laser by using the phase modulated technique

Shu-Tao Dai(戴殊韬), Hong-Chun Wu(吴鸿春), Fei Shi(史斐), Jing Deng(邓晶), Yan Ge(葛燕), Wen Weng(翁文), Wen-Xiong Lin(林文雄)
Chin. Phys. B . 2018, 27(5): 054212 . **doi:** 10.1088/1674-1056/27/5/054212

Suppressing the preferential σ-polarization oscillation in a high power Nd：YVO_4 laser with wedge laser crystal

Zheng Yao-Hui, Zhou Hai-Jun, Wang Ya-Jun, Wu Zhi-Qiang
Chin. Phys. B . 2013, 22(8): 084207 . **doi:** 10.1088/1674-1056/22/8/084207

330-W single-frequency retrievable multi-tone monolithic fiber amplifier

Wang Xiao-Lin, Zhou Pu, Leng Jin-Yong, Du Wen-Bo, Xu Xiao-Jun
Chin. Phys. B . 2013, 22(4): 044205 . **doi:** 10.1088/1674-1056/22/4/044205

A 3-kHz Er:YAG single-frequency laser with a 'triple-reflection' configuration on a piezoelectric actuator*

Shuai Huang(黄帅)[1,2], Qing Wang(王庆)[1,2,†], Meng Zhang(张濛)[1,2], Chaoyong Chen(陈朝勇)[1,2], Kaixin Wang(王凯鑫)[1,2], Mingwei Gao(高明伟)[1,2], and Chunqing Gao(高春清)[1,2]

[1] *School of Optics and Photonics, Beijing Institute of Technology, Beijing* 100081, *China*

[2] *Key Laboratory of Information Technology, Ministry of Industry and Information Technology, Beijing Institute of Technology, Beijing* 100081, *China*

(Received 8 March 2020; revised manuscript received 16 April 2020; accepted manuscript online 19 May 2020)

A novel Er:YAG laser system operating at 1645 nm with high pulse-repetition-frequency (PRF) of kHz level is demonstrated. A ring cavity with double gain medium end-pumped by two fiber lasers is utilized to obtain high pulse energy. A novel 'triple-reflection' configuration on a piezoelectric actuator (PZT) is adopted to achieve high-repetition-rate at 3-kHz operation with the ramp-fire locking method. Single frequency pulses with maximum average power of 18.3 W at 3 kHz are obtained, and the pulse duration time is 318 ns. The full line width at half maximum (FWHM) of the pulses measured by the heterodyne technique is 1.71 MHz at 3 kHz. To the best of our knowledge, this is the highest PRF single-frequency laser pulses achieved based Er:YAG gain medium.

Keywords: Er:YAG, injection-seeded, single-frequency, high pulse-repetition-frequency

PACS: 42.55.Xi, 42.60.Gd, 42.60.By **DOI:** 10.1088/1674-1056/ab9441

1. Introduction

Single-frequency Er-droped laser system emitting around 1.6 μm is widespread applied in wind measurement Doppler Lidar, coherent imaging lidars.[1–3] In these applications, output pulses with high pulse energy, high pulse repetition frequency, and narrow line-width are essential to realize a long-distance measurement.[4] An effective way to achieve such laser pulses is to utilize a single longitudinal mode laser output with narrow line-width to pull a high energy *Q*-switched slave cavity.[5–8]

The last decade has seen the rapid development of the Er:YAG lasers at 1.6 μm for their operation in the atmospheric window and eye-safe wavelength. In 2005, Setzler *et al.* obtained a *Q*-switched Er:YAG laser with pulse energy of 16 mJ under a pulse repetition rate of 250 Hz at 1645 nm.[9] In 2010, Kim *et al.* reported a fiber laser pumped, Er:YAG laser at 1617 nm with a pulse energy of 11.6 mJ at a PRF of 250 Hz.[10] In 2014, Wang *et al.* demonstrated a 200 Hz, *Q*-switched, injection-seeded Er:YAG laser with a single-frequency pulse energy of 4.75 mJ.[11] In 2015, Yao *et al.* presented a 1645-nm Er:YAG single frequency laser seeded by a nonplanar ring oscillator (NPRO), they got 2.9-mJ pulse output with a pulse width of 160 ns.[12] In 2019, Zhang *et al.* reported an Er:YAG single frequency laser with average power of 8.4 W at PRF of 2 kHz.[13] Besides, two pumping sources pumped double crystals laser system was also reported in 2019 and 2020. They achieved 20.3-mJ, 110-ns single-frequency pulse output at 200 Hz[14] and 28.6 mJ, 159 ns.[15] For the application of a wind Lidar, the figure of merit (FOM) defined by the pulse energy and the square root of PRF, can reflect the detection capability. High PRF can not only reduce the time of one scan cycle when it is necessary to obtain samples of dense space, but also improve the signal-to-noise ratio (SNR) of the measurement.[1]

In this paper, a PRF as high as 3-kHz single-frequency Er:YAG laser is demonstrated. The output pulse energy is 6.1 mJ with a pulse duration of 318 ns, and the average power is 18.3 W. The FWHM of the laser pulse is 1.71 MHz, which is 1.22 times Fourier transform limited. To achieve laser output pulses with high PRF, a novel 'triple-reflection' architecture in the cavity is designed. To our knowledge, 3 kHz is the highest repetition frequency, and 18.3 W is the highest output average power achieved from an injection-seeded single-frequency Er:YAG laser. This high PRF single frequency laser is an ideal laser source for coherent Lidar system.

2. Experimental setup

The laser system consists of three parts: the seed laser, an 'M-shaped' slave ring oscillator, a control system (see Fig. 1).

The seed laser is an LD pumped Er:YAG NPRO with 700-mW single-frequency output power. An isolator is set to protect the NPRO to prevent the feedback leaked from the amplifier. By rotating the half-wave plate, before passing through the polarizing beam splitter (PBS), the seed laser is divided

*Project supported by the National Key Research and Development Program of China (Grant No. 2017YFB0405203) and the National Natural Science Foundation of China (Grant No. 61627821).

†Corresponding author. E-mail: qingwang@bit.edu.cn

© 2020 Chinese Physical Society and IOP Publishing Ltd

into two parts: the one part (500 mW) is p-polarized, injected into the slave cavity for seed with p-polarization has much sharper resonance signal which has a benefit for injection seeding,[16] the other part (200 mW) is used as the reference for heterodyne beating with single frequency pulses. M9, M10 are 45° flat mirrors for folding the seed laser into the salve resonator.

A *Q*-switched Er:YAG ceramic laser is employed as the slave laser which is an 'M-shape' ring cavity and the total length of the cavity is 2.1 m. The whole slave laser composed of six mirrors. Two 45° dichroic flat mirrors M1, M3 are anti-reflection coated at pumping wavelength of 1532 nm and coated with high reflection at lasing wavelength of 1645 nm M5, M6 are 0° flat mirrors with high reflection at lasing wavelength. M5 is mounted upon the piezoelectric actuator (PZT) for finely adjusting the length of the cavity. M6 is used for increasing the number of reflections to 3 bounces on the mirror M5 to achieve high repetition frequency operation. M2 and M4 are dichroic curved mirrors with the same radius curvature of 750 mm, where M2 is a pump mirror and M4 is utilized as an output coupler with a transmittance of 20% at 1645 nm. Two fiber lasers (ELR-30-1532-LP IPG Inc) operated at 1532 nm are employed as the pump source which have line width less than 0.2 nm and total 64 W of output. Compared with LD, fiber laser can provide higher pumping rate and better beam quality. For the purpose of reducing the energy transfer up-conversion (ETU),[17] we choose two Er:YAG ceramics with doping concentration of 0.25 at.% and dimensions of 6 mm in length as the gain medium whose both sides are antireflection coated ranging from 1532 nm to 1645 nm. Both ceramics are wrapped with indium foil and tightly mounted in a copper heat sink whose temperature is maintained at 18 °C by thermoelectric cooler (TEC). The lens f1 and f3 are both used for focusing pump beam to match with laser to get higher optical efficiency. A fused silica AOM (MQH068 Gooch Inc) is used to produce *Q*-switched operation. The seed laser is injected into the slave cavity through the first diffraction order of AOM at Bragg angle, and its laser frequency is shifted with 40.8 MHz.

We adopt 'ramp-fire' technique to achieve injection-seeded operation. A control program is written to realize the resonance matching for seed laser and slave cavity. Lens f4 focuses the seed beam for seed mode matching with the slave laser. A photodiode (PD1 in Fig. 1) is adopted to detect the leaking resonance signal. Length of the slave cavity varies with the vibration of PZT to match the seed laser. The AOM is triggered when the resonance signal peak is detected. Then, single-frequency pulses are obtained.

The mixed signal of single frequency pulse and seed laser (second part) are sent to a photodiode and sampled by an oscilloscope (TDS5025B, Tektronix) to measure the results of injection-seeding and the line width. The fused silica wedge and M11 (uncoated fused silica) is used to reflect a small proportion of the pulsed laser with high energy to beat with the seed laser.

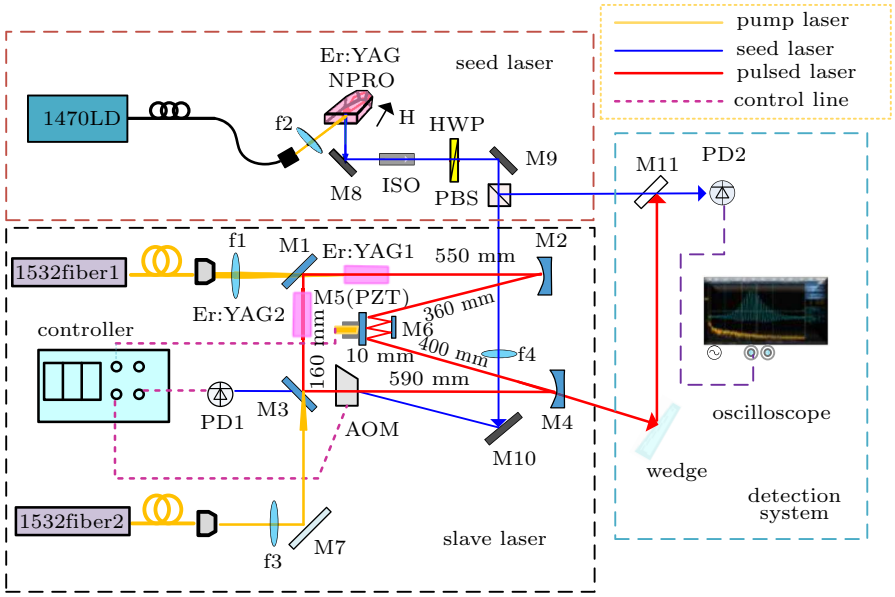


Fig. 1. Lay out of the novel Er:YAG laser system. PD: photo detector; PBS: polarization beam splitter; HWP: half wave plate; ISO: isolator; LD: laser diode; AOM: acousto–optic modulator; PZT: piezoelectric ceramic transducer.

3. Result and discussion

The main parameters of PZT are as follows: voltage U, capacitance C, motion frequency f, the average electrical power which can be expressed as

$$P \approx f \cdot C \cdot U^2, \tag{1}$$

where, the rated electrical power (P) and the capacitance (C),

are both the fixed properties of the PZT, and are not changed by other factors. Therefore, the motion frequency (f) is negatively related to the voltage (U) applied to PZT. If the motion frequency (f) increases, U must be reduced, which will shorten the scanning range of PZT. Meanwhile, the number of resonance signal peaks decreases that will lead to unstable injection locking.[13] In this work, a novel 'triple-reflection' structure is proposed. The most important element of this structure is M6 in Fig. 1, which is used to ensure that the laser reflects on M5 mounted upon PZT three bounces. The displacement of the optical path can be increased during the movement of the PZT, which implies that the required voltage of the PZT can be reduced at the same optical path displacement. According to Eq. (1), under the same driving power of the PZT, the lower voltage means higher operating frequency of the PZT, and the lower voltage can also reduce the hysteresis effect of the PZT and improve the stability of the laser system as well. Therefore, we design the 'triple-reflection' configuration to achieve high repetition operation. The displacement of the PZT can be increased during the movement of PZT, which means that a lower required voltage applied to the PZT with the same displacement range.

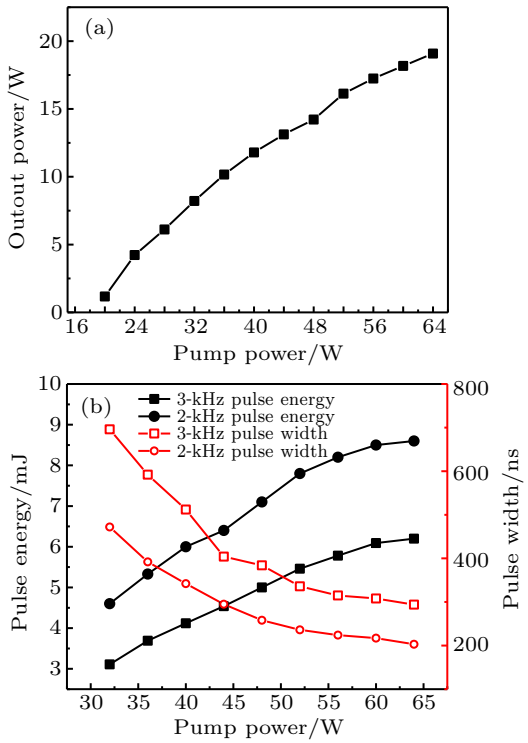


Fig. 2. (a) Output power in the CW mode. (b) Pulse energy and pulse width at the PRF of 2 kHz and 3 kHz in the Q-switch operation.

We firstly investigate the free running operation (without Q-switcher) of the slave cavity. Continuous wave (CW) power properties of the laser system are demonstrated in Fig. 2(a), under full pump power, maximum CW output power is 19.08 W. Figure 2(b) shows the Q-switched pulse properties at the PRF of 2 kHz and 3 kHz without seed injection. The maximum pulse energies are 8.6 mJ, 6.1 mJ, and pulse widths are 203 ns, 294 ns, respectively.

The essence of injection-seeding is the competition between the seed mode and the free oscillation mode in the resonator. Therefore, the key factors for the success of injection-seeding are the initial values of seed mode and oscillation mode of the slave cavity, and the speed of extraction gain of the seed mode and free oscillation mode. To achieve injection-seeding successfully, the seed beam must have a certain intensity, which can suppress the free oscillation mode in the resonant cavity, while the seed laser mode is dominant. Based on the laser equations set up by Kurtz,[18] the equation describing the phase can be written as

$$\frac{\mathrm{d}\phi(t)}{\mathrm{d}t} + \omega_1 - \omega_0 = -\gamma_e \frac{E_1(t)}{E(t)} \sin[\phi(t) - \phi_1(t)], \tag{2}$$

where ω is the natural radian frequency which is driven by the seed signal with radian frequency ω_1 and γ_e is the rate of out coupling, which can be described as

$$\gamma_e = \ln(1/R_0) \cdot \Delta f_{\mathrm{FSR}}, \tag{3}$$

and R is the reflectivity of the output couple, Δf_{FSR} is the free spectral range of the slave cavity, for a ring laser, the $\Delta f_{\mathrm{FSR}} = c/nL$. Assuming that equation (2) can be solved in the steady state, the frequency and amplitude of the resonator are constant over time and making use of that $|\sin\phi| \leq 1$

$$\Delta\nu = \frac{|\omega_1 - \omega_0|}{2\pi} = |\nu_1 - \nu_0| \leq \gamma_e \frac{E_1}{E_0} = \frac{\ln(1/R_0)C}{2\pi L}\sqrt{\frac{I_1}{I_0}}. \tag{4}$$

The relationship between the maximum frequency detuning to achieve injection seeding and the cavity parameters can be obtained from Eq. (4). Frequency detuning versus light intensity of seed laser at different cavity lengths is shown in Fig. 3(a). This demonstrates that the longer the slave cavity is, the smaller the maximum frequency detuning allowed by the injection seeding laser is. But for a Wind Lidar, a longer cavity is necessary to get a longer pulse width, and under the same cavity length, the free spectral region of the ring cavity is twice that of the standing wave cavity, which means that the ring cavity can make more effective use of the energy of seed light. Therefore, we comprehensively consider that the resonator is designed as a ring laser with a length of 2 m. Frequency detuning versus light intensity of seed laser at different output coupler transmissions is shown in Fig. 3(b), from which we can know that the higher the transmissivity of the output coupler, the greater the frequency detuning of the frequency locking that can be realized by the same seed power,

but, too high transmittance will reduce the output efficiency. So that the transmittance of the output coupler is 20%. When the cavity parameters are determined, increasing the power of the injected seed laser can effectively improve the frequency detuning of the injection seeding. For high PRF operation, the resonance peak is hard to be detected, so we lock the cavity's length of slave laser to the wavelength of the seed laser to minimize the difference with free-running operation. Besides, a higher seed laser (500 mW) is used to inject into the cavity to ensure high success rate of injection-seeding. Figure 3(c) shows the detected resonance signal. The detected resonance peak (channel 2 in Fig 3(c)) is sufficiently higher to achieve the injection-seeding operation. The frequency of PZT's voltage (channel 1 in Fig. 3(c)) shows that pulse is operated up to the PRF of 3 kHz. The *Q*-switched gate (channel 3 in Fig. 3(c)) is open at the resonance peak so the single-frequency pulses can be quickly built up from the seed laser. Finally, we used 10-V voltage loaded the PZT to achieve 3-kHz operation (previously the same voltage was up to 2 kHz).

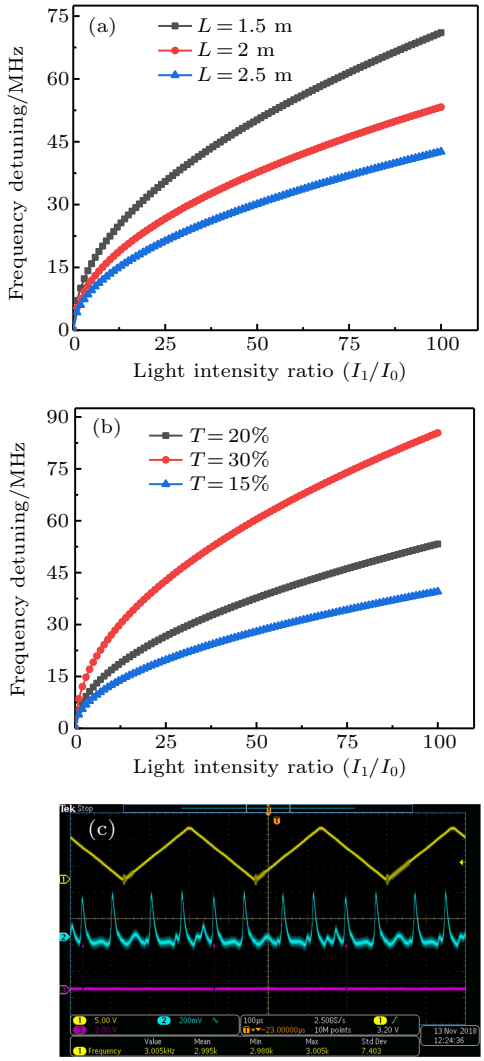


Fig. 3. (a) Frequency detuning *versus* light intensity of seed laser with different cavity lengths. (b) Frequency detuning *versus* light intensity of seed laser at different output coupler transmissions. (c) The detected resonant signal at 3 kHz when scanning the length of the slave cavity.

The output single-frequency pulse properties of the Er:YAG laser at the PRFs of 2 kHz and 3 kHz *versus* the pump power are demonstrated in Fig. 4(a). Maximum output energy is 8.2 mJ, 6.1 mJ, and the pulse width is 214 ns and 318 ns, respectively. Figure 4(b) shows the pulse build-up time of the *Q*-switched laser pulses with and without seed-injection at the PRFs of 3 kHz. With the increase of the pump power, the pulse build-up time is shortened at the same pump power, it is also shortened after the seed laser injected into the cavity for the power of the seed laser is much higher than spontaneous radiation, the pulse is much easier to build-up.

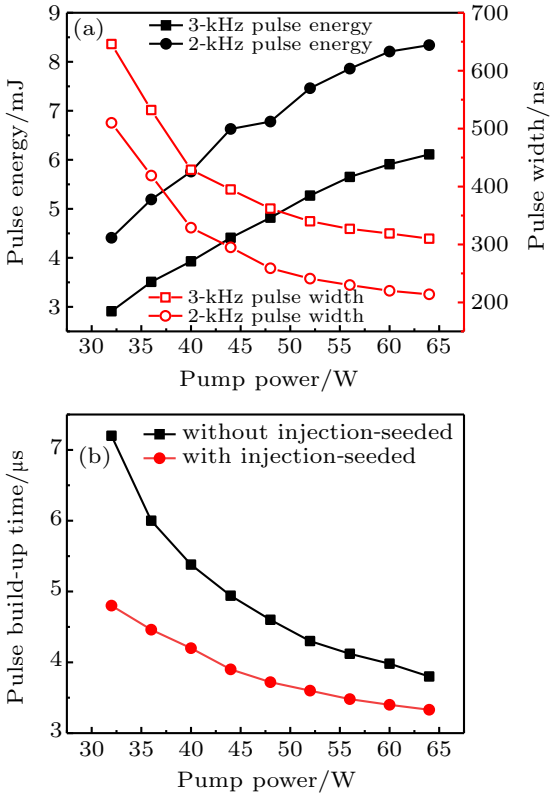


Fig. 4. (a) The output properties of single-frequency pulse *versus* pump power. (b) Build-up time before and after injection-seeding at the PRFs of 3 kHz *versus* the pump power.

An InGaAs photodetector (EOT5000, EOT Inc.) is used to detect the pulses profile after injection-seeded, and the profile is shown in Fig. 5(a), a smooth profile illustrates that the pulses operating at 3 kHz are in single-frequency operation. We measure the spectrum of the single-frequency pulses by heterodyne technique to inspect the successful probability of injection-seeding and the spectrum of the single-frequency pulses could be retrieved from it. The spectrum intensity profile is provided for the analysis of beating signal by fast-Fourier transform (FFT). The central frequency of the single-frequency pulse is calculated at 36.56 MHz, FWHM is 1.71 MHz (shown in Fig. 5(b)), which is 1.22 times Fourier transform limited (318 ns, Gaussian pulse shape). And figure 5(c) shows the heterodyne beating signal at 3 kHz.

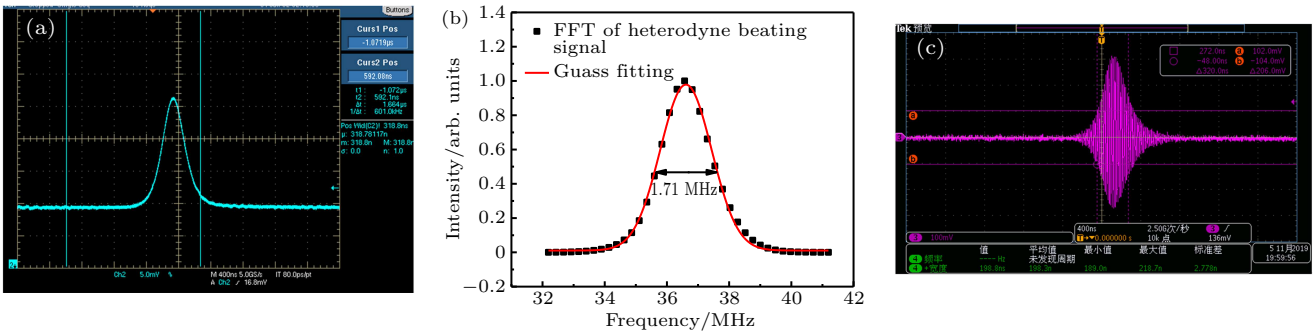


Fig. 5. (a) The pulse temporal profiles of single-frequency pulse at a PRF of 3 kHz. (b) The corresponding spectral characteristics of the single-frequency pulses. (c) The heterodyne beating signal at 3 kHz.

The beam profiles of single-frequency pulses are measured in different positions by using a PY-III camera (Spricon Inc.) under the maximum output (Fig. 6(a)). The M^2 factors are 1.51 and 1.54 in x and y directions. Figure 6(b) demonstrates the single-frequency pulse energy fluctuation at 3 kHz within 30 minutes, whose RMS is less than 1.23%.

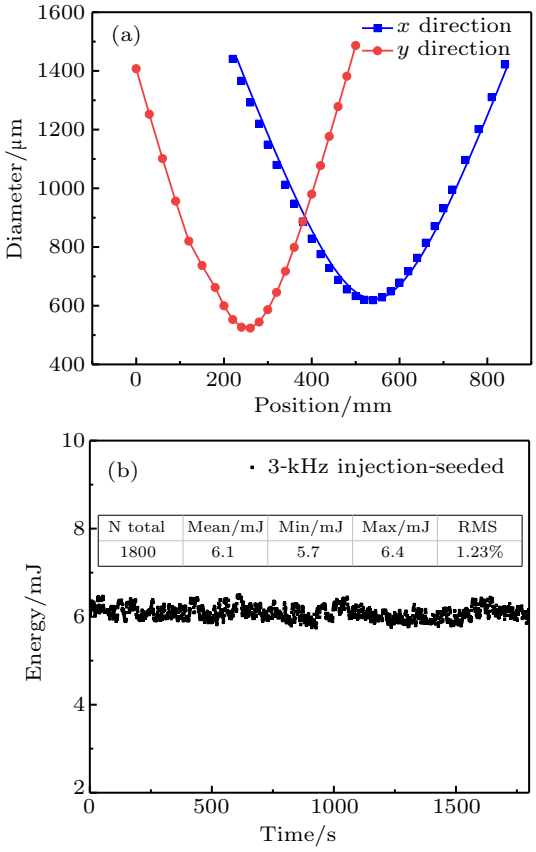


Fig. 6. Characteristics of 3-kHz single-frequency pulse: (a) beam quality and (b) pulse energy fluctuation.

4. Conclusion

In conclusion, a single-frequency Er:YAG laser with high PRF and high pulse energy at 1645 nm is demonstrated. An 'M-shape' ring resonator with two Er:YAG gain mediums is utilized to achieve high pulse energy, and a 'triple-reflection' configuration is designed to ensure the success of injection-seeding at high PRF. The single-frequency pulses energy up to 8.2 mJ and 6.1 mJ at a PRF of 2 kHz and 3 kHz with the corresponding pulse widths of 214 ns, 318 ns are obtained. At the PRF of 3 kHz, the line width is almost Fourier limited (1.71 MHz), the measured M^2 factors are 1.51 and 1.54 in x and y directions, respectively and the stability of the maximum output pulse energy is less than 1.23% (RMS) measured within 30 minutes. According to what we know, this is the highest PRF single frequency laser pulse achieved based on Er:YAG gain medium. We believe the laser system in this work is an ideal laser source for fast scan wind measurement Doppler Lidar system.

References

[1] Malm A I R, Hartman R and Stoneman R C 2004 *Opt. Soc. Am.* **2004** 356

[2] Mizutani K, Ishii S, Aoki M, Iwai H, Oysuka R, Fukuoka H, Isikawa T and Sato A 2018 *Opt. Lett* **43** 202

[3] Hannon S, Barr K, Novotny J, Bass J, Oliver A and Anderson M 2008 *European Wind Energy Conference and Exhibition*, March, 2008, Brussels, Belgium, pp. 1–7

[4] Henderson S W, Hale C P, Magee J R, Kavaya M J and Huffaker A V 1991 *Opt. Lett.* **16** 773

[5] Cao X Z, Li P L, Wang Z Y and Liu Q 2019 *Chin. Phys. Lett.* **36** 124201

[6] Henderson S W, Hale C P, Magee J R, Kavaya M J and Huffaker A V 1991 *Opt. Lett.* **16** 773

[7] Koch G J, Deyst J P and Storm M E 1993 *Opt. Lett.* **18** 1235

[8] Yu J, Singh U N, Barnes N P and Petros M 1998 *Opt. Lett.* **23** 780

[9] Setzler S D, Francis M P, Young Y E, Konves J R and Chicklis E P 2005 *IEEE J. Quantum Electron.* **11** 645

[10] Kim J, Mackenzie J, Sahu J and Clarkson W, 2010 *7th EMRS DTC Technical Conference*, 2010, Edinburgh, UK, p. B1

[11] Wang R, Ye Q, Zheng Y, Gao M W and Gao C Q 2014 *Proc. SPIE* **8959** 89590F

[12] Yao B Q, Deng Y, Dai T Y, Duan X M, Jun Y L and Wang Y Z 2015 *Quantum Electron.* **45** 709

[13] Zhang Y X, Gao C Q, Wang Q, Na Q X, Gao M W, Zhang M and Huang S 2019 *Laser Phys. Lett.* **16** 115002

[14] Shi Y, Gao C Q, Wang S, Li S H, Song R, Zhang M, Gao M W and Wang Q 2019 *Opt. Express* **27** 2671

[15] Li S H, Wang Q, Song R, Hou F F, Gao M W and Gao C Q 2020 *Chin. Opt. Lett.* **18** 031401

[16] Na Q X Gao C Q, Wang Q, Zhang Y X, Gao M W, Zhang M and Wang Y J 2017 *Laser Phys. Lett* **14** 085002

[17] Kim J W, Shen D Y, Sahu J K and Clarkson W A 2009 *IEEE J. Sel. Top. Quantum Electron.* **15** 361

[18] Kurtz R M, Pradhan R D, Tun N, Aye T M, Savant G D, Jannson T P and DeshazerLG 2005 *IEEE J. Quantum Electron.* **11** 578